Gradient field approximation: Application to registration in image processing

Carole Le Guyader, Christian Gout, Anne-Sophie Macé, Dominique Apprato

Gradient field approximation: application to registration in image processing

Carole Le Guyader[1] Christian Gout[1] Anne-Sophie Macé[1] and Dominique Apprato[2]

[1]: *INSA de Rouen, Laboratoire de Mathématiques de l'INSA, Avenue de l'Universite, 76801 St Etienne du Rouvray cedex France*

[2]: *Université de Pau, LMA-CNRS, UFR Sciences et Technologies de la Côte Basque, All. Parc Montaury, 64600 Anglet, France.*

Abstract

We study a spline-based approximation of vector fields in the conservative case (the gradient vector field derives from a potential function). We introduce a minimization problem on a Hilbert space for which the existence and uniqueness of the solution is given. We apply this approach to a registration process in image processing.

Keywords:
Registration, Image processing, Approximation, smoothing problems, vectorial splines, convergence, Sobolev space, conservative vector fields.

AMS subject classification: 41A15, 41A25, 68U10.

1. Introduction

In image processing, registration is an important task since it allows to compare a subject/time-variant template image T with an unbiased reference image R. More precisely, given a reference R and a template T defined on an image domain Ω, the goal is to find a smooth invertible transformation to map T into an image similar to R. For images of the same modality, a well-registered template has geometric features and intensity distribution matched with the reference.
An extensive overview of registration techniques can be found in [33]. These can be partitioned into two classes: parametric and non-parametric ones. In the non-parametric methods (our framework), the problem is phrased as a functional minimization whose unknown is the displacement vector field u. The introduced functional combines a distance measure component $\mathcal{D}[R, T, u]$ and a smoother on the displacement vector field $\mathcal{S} = \mathcal{S}[u]$ to remove the ill-posed character of the problem.
Thus we take as input in our problem the obtained vector field after applying a classical registration process (see for instance [9], [12], [14], [24], [18], [19] or [20]). In the examples related to image registration, the reference system is centred on the top left corner, the x-direction (first component) corresponds to the column direction and the y-direction (second component) to the row direction. The y-direction points downwards.

The starting point of this work is the conservative vector field approximation, that is to say, when the studied vector field derives from a potential (real-valued function). This problem occurs for instance in electromagnetism, meteorology, medical imaging or radar image analysis. Here, we do not want to compute a potential that could generate the vector field data. We only want to get a global approximation of the vector field dataset on a bounded domain, taking into account in the modelling that this approximation derives from a potential. This implies that the components of the computed vector field are an isotropic approximation of the vector field dataset. Furthermore, contrary to interpolation methods, we prefer to fit the vector field dataset in the case of realistic data (when the number of vectors is large or with noisy data). To achieve this (see Section 2), we introduce a minimization problem defined as a regularized least-square problem formulated on a Sobolev space of potentials. Obviously, this problem has an infinity of solutions, but we derive from it a problem expressed in terms of the gradient vectors. We prove that the associated problem in terms of vectors has a unique solution which is the corresponding approximation of the vector field dataset. In Section 3, we give a convergence result when the number of vectors increases to infinity. We use in Section 4 a finite element method to discretize the approximation problem and provide bidimensional experimental results on both synthetic data and real data.

Before depicting the proposed model, we briefly review some prior related works. In [2], Amodei and Benbourhim introduce a new family $P_{\alpha,\beta}$ of spline minimization problems for vector fields defined by

$$P_{\alpha,\beta} \begin{cases} min \left(\alpha \int_{\mathbb{R}^2} ||\nabla \operatorname{div} V||^2 \, dx\, dy + \beta \int_{\mathbb{R}^2} ||\nabla \operatorname{rot} V||^2 \, dx\, dy \right), \\ V \in \chi \text{ and } V(X_i) = V_i,\ i \in 1, \cdots, N, \end{cases}$$

where $V = (u, v)$ is a two component vector function, χ is the Beppo-Levi space $D^{-2}L^2(\mathbb{R}^2) \times D^{-2}L^2(\mathbb{R}^2)$, $X_i = (x_i, y_i)$ are the interpolation points, and $V_i = (u_i, v_i)$ are data values. The use of the divergence and rotational operators allows to couple the components of V, which is very useful when tracking geophysical fluid flows for instance. It also allows to handle the variations in the magnitudes of the divergent and rotational parts of the flow.

In [38], Xu and Prince devise a new static external force called Gradient Vector Flow (GVF) in order to address both the problem of initialization and slow/poor convergence near boundaries with strong concavities in the context of image segmentation. The main idea behind this model is to increase the capture range of the edge-map-related vector field and to make the contour evolve toward the desired boundaries where classical methods would fail. This extrapolation step is phrased in terms of a functional minimization problem. Denoting Df to be the gradient vector field of an edge map (this field is only significant near boundaries and is almost null in homogeneous regions) and $w = (u, v)$ to be the expected extrapolated vector field, Xu and Prince propose to minimize the following functional:

$$E(w) = \mu \int_\Omega \left(u_x^2 + u_y^2 + v_x^2 + v_y^2 \right) dx\, dy + \int_\Omega ||Df||^2 ||w - Df||^2 \, dx\, dy,$$

with μ a tuning parameter, Ω, a bounded open subset of $\mathbb{R}^2$, $||\cdot||$ denoting the Euclidean norm in $\mathbb{R}^2$, and with the notation $u_x = \frac{\partial u}{\partial x}$. The energy E is thus designed such that when $||Df||$ is large, it is minimized by setting $w = Df$, and when $||Df||$ is small, the resulting w is smooth and slowly varying. The Euler-Lagrange equations are computed and lead to a decoupled linear partial

differential equation system to be solved. Numerically, these equations are solved by a gradient descent method, and one obtains the following system:

$$\begin{cases} \frac{\partial u}{\partial t} = \mu \Delta u - 2||Df||^2(u - f_x), \\ \frac{\partial v}{\partial t} = \mu \Delta v - 2||Df||^2(v - f_y). \end{cases}$$

In [22], Jifeng et al. propose to improve the diffusion properties of the GVF force field. They obtain a new force by replacing the Laplacian operator used in the GVF model by its diffusion term in the normal direction that is, the 'normalized' infinity Laplacian operator. Numerically, the authors thus solve the following decoupled partial differential equation system:

$$\begin{cases} \frac{\partial u}{\partial t} = \mu \; u_{NN} - 2||Df||^2(u - f_x), \\ \frac{\partial v}{\partial t} = \mu \; v_{NN} - 2||Df||^2(v - f_y), \end{cases}$$

where $u_{NN} = \frac{u_x^2 u_{xx} + 2u_x u_y u_{xy} + u_y^2 u_{yy}}{||Du||^2}$.
Unlike the GVF model, their new field (called NGVF) is anisotropic.

More recently, Le Guyader and Guillot investigate in [26] a new Gradient-Vector-Flow-inspired external vector field for active contour models, deriving from the edge map of a given image and allowing to increase the capture range. Contrary to the above related works, the number of unknowns is reduced to a single one v by assuming that the expected vector field is the gradient vector field of a scalar function. The model is phrased in terms of a functional minimization problem comprising a data fidelity term and a regularizer based on the supremum norm of Dv. The minimization is achieved by solving a second order singular degenerate parabolic equation. A comparison principle as well as the existence/uniqueness of a viscosity solution together with regularity results are established.

Another application in image processing dedicated to vector field interpolation is addressed in [11]. Chessel et al. develop an axiomatic approach of vector field interpolation, which is useful as a feature extraction preprocessing step. More precisely, the goal is to seek an orientation field that captures the geometrical features of a given image. In this prospect, the authors propose an analysis similar to [1], [10] and single out two operators: the curvature operator and the Absolutely Minimizing Lipschitz Extension.

The originality of this work consists in considering that the vector field derives from a potential (conservative vector field). We also present a rigorous study of existence-uniqueness of the solution of the problem phrased as an energy minimization and a convergence result is given.

From our knowledge, our approach is the first one of this kind. Moreover, in our approach, we propose a method easy to implement and parallelize, using classical tools like the least square method and the finite element method (for the discretization).

2. Modelling

2.1. Notations

Let Ω be a non-empty connected bounded open subset of $\mathbb{R}^n$ with Lipschitz boundary. Let $A = \left\{a_i\right\}_{i=1,\cdots,N}$ be an ordered set of N points of $\bar{\Omega}$ which contains a P^{m-1}-unisolvent subset.

Let also $\left\{w_i\right\}_{i=1,\cdots,N}$ be a set of N vectors of $\mathbb{R}^n$ which corresponds to the vector field dataset. We aim at finding a function $\Phi : \bar{\Omega} \to \mathbb{R}$ smooth enough such that for $i = 1, \cdots, N$,

$$\nabla\Phi(a_i) \simeq w_i \in \mathbb{R}^n.$$

Let us denote by ρ the operator defined by:

$$\rho : \left\{ \begin{array}{l} H^m(\Omega, \mathbb{R}^n) \to (\mathbb{R}^n)^N \\ v \mapsto \rho(v) = (v(a_1), \cdots, v(a_N))^T. \end{array} \right. \tag{1}$$

Let us assume that $m > \frac{n}{2}$ so that the following Sobolev 's embeddings hold:

$$H^m(\Omega, \mathbb{R}^n) \circlearrowleft \mathcal{C}^0(\bar{\Omega}, \mathbb{R}^n) \tag{2}$$

$$H^{m+1}(\Omega, \mathbb{R}) \circlearrowleft \mathcal{C}^1(\bar{\Omega}, \mathbb{R}) \tag{3}$$

One sets $\forall \xi \in (\mathbb{R}^n)^N$ and $\forall \eta \in (\mathbb{R}^n)^N$,

$$\langle \xi, \eta \rangle_N = \sum_{i=1}^{N} \langle \xi_i, \eta_i \rangle_n,$$

where $\langle \cdot, \cdot \rangle_n$ denotes the Euclidean scalar product in $\mathbb{R}^n$ and $\forall \xi \in (\mathbb{R}^n)^N$, $\langle \xi \rangle_N = \langle \xi, \xi \rangle_N^{\frac{1}{2}}$.

2.2. The fitting model

We first introduce a regularized least-square problem defined on a space of potentials (real-valued functions) to fit the vector field dataset. For any $\epsilon > 0$, we introduce the functional $\mathcal{J}_\epsilon$ defined as follows:

$$\mathcal{J}_\epsilon : \left\{ \begin{array}{l} H^{m+1}(\Omega, \mathbb{R}) \to \mathbb{R} \\ \\ v \mapsto \langle \rho(\nabla v) - w \rangle_N^2 + \epsilon |v|^2_{m+1,\Omega,\mathbb{R}}, \end{array} \right. \tag{4}$$

where $w = (w_1, \cdots, w_N)^T \in (\mathbb{R}^n)^N$ is the vector field dataset and $|\cdot|_{m+1,\Omega,\mathbb{R}}$, the semi-norm on $H^{m+1}(\Omega, \mathbb{R})$.

This kind of approach is related to the smoothing D^m-splines for surface approximation introduced by Arcangéli [5] (see also Duchon [15] for a general introduction or Gout [21], and López de Silanes and Arcangéli [29, 30] for convergence results). We consider the following fitting problem using potentials:

$$\left\{ \begin{array}{l} \text{Search for } \sigma_\epsilon \in H^{m+1}(\Omega, \mathbb{R}) \text{ such that} \\ \\ \forall v \in H^{m+1}(\Omega, \mathbb{R}),\ \mathcal{J}_\epsilon(\sigma_\epsilon) \leq \mathcal{J}_\epsilon(v), \end{array} \right. \tag{5}$$

where $\mathcal{J}_\epsilon$ is defined in (4). Obviously, the minimization problem (5) does not have a unique solution, the potential function σ_ϵ being defined up to a constant.
So, in order to overcome the lack of uniqueness, we introduce the following problem expressed in terms of the gradients of the potentials: as ϵ is a positive arbitrary parameter and as $|.|_{m+1,\Omega,\mathbb{R}}$ and $|\nabla.|_{m,\Omega,\mathbb{R}^n}$ are equivalent in $H^{m+1}(\Omega,\mathbb{R})$, we derive from problem (5), the following problem of minimization:

$$\left\{\begin{array}{l} \text{Search for } \sigma_\epsilon \in H^{m+1}(\Omega,\mathbb{R}) \text{ such that } \forall v \in H^{m+1}(\Omega,\mathbb{R}), \\ \langle \rho(\nabla\sigma_\epsilon) - w\rangle_N^2 + \epsilon|\nabla\sigma_\epsilon|^2_{m,\Omega,\mathbb{R}^n} \leq \langle \rho(\nabla v) - w\rangle_N^2 + \epsilon|\nabla v|^2_{m,\Omega,\mathbb{R}^n}. \end{array}\right. \tag{6}$$

This formulation leads to the following problem associated to problem (6). To state this new problem, we first define the following functional denoted by $\mathcal{F}_\epsilon$:

$$\mathcal{F}_\epsilon : \left\{\begin{array}{l} H^m(\Omega,\mathbb{R}^n) \to \mathbb{R} \\ f \mapsto \langle \rho(f) - w\rangle_N^2 + \epsilon|f|^2_{m,\Omega,\mathbb{R}^n}, \end{array}\right. \tag{7}$$

and we consider the following problem stated by:

$$\left\{\begin{array}{l} \text{Search for } u_\epsilon \in H^m(\Omega,\mathbb{R}^n) \text{ such that} \\ \forall v \in H^m(\Omega,\mathbb{R}^n),\ \mathcal{F}_\epsilon(u_\epsilon) \leq \mathcal{F}_\epsilon(v). \end{array}\right. \tag{8}$$

2.3. Existence and uniqueness results

We have the following theorem:

Theorem 2.1. *Problem (8) is equivalent to the following variational problem:*

$$\left\{\begin{array}{l} \textit{Search for } u_\epsilon \in H^m(\Omega,\mathbb{R}^n) \textit{ such that} \\ \forall v \in H^m(\Omega,\mathbb{R}^n),\ \langle \rho(u_\epsilon), \rho(v)\rangle_N + \epsilon(u_\epsilon, v)_{m,\Omega,\mathbb{R}^n} = \langle w, \rho(v)\rangle_N. \end{array}\right. \tag{9}$$

Proof

Let us denote by a the mapping defined by:

$$a : \left| \begin{array}{l} H^m(\Omega,\mathbb{R}^n) \times H^m(\Omega,\mathbb{R}^n) \to \mathbb{R} \\ (u,v) \mapsto \langle \rho(u), \rho(v)\rangle_N + \epsilon\,(u,v)_{m,\Omega,\mathbb{R}^n} \end{array}\right. \tag{10}$$

with $(u,v)_{m,\Omega,\mathbb{R}^n} = \sum_{|\alpha|=m} \int_\Omega \langle D^\alpha u, D^\alpha v\rangle_n \, dx$, and by L the mapping defined by:

$$L : \left| \begin{array}{l} H^m(\Omega,\mathbb{R}^n) \to \mathbb{R} \\ v \mapsto \langle w, \rho(v)\rangle_N \end{array}\right. . \tag{11}$$

Let us notice that $\forall v \in H^m(\Omega, \mathbb{R}^n)$, $\mathcal{F}_\epsilon(v) = a(v,v) - 2L(v) + \langle w \rangle_N^2$.

Problem (8) is equivalent to:

$$\left\{ \begin{array}{l} \text{Search for } u_\epsilon \in H^m(\Omega, \mathbb{R}^n) \text{ such that} \\ \forall v \in H^m(\Omega, \mathbb{R}^n), \forall \mu \in \mathbb{R},\ \mathcal{F}_\epsilon(u_\epsilon) \leq \mathcal{F}_\epsilon(u_\epsilon + \mu v) \end{array} \right. . \tag{12}$$

Let u_ϵ be a solution of (12). Then $\forall v \in H^m(\Omega, \mathbb{R}^n)$ and $\forall \mu \in \mathbb{R}$, $\mathcal{F}_\epsilon(u_\epsilon) \leq \mathcal{F}_\epsilon(u_\epsilon + \mu v)$. Using the bilinearity and symmetry of the mapping a, and the linearity of the mapping L, one has:

$$\mathcal{F}_\epsilon(u_\epsilon + \mu v) = \mathcal{F}_\epsilon(u_\epsilon) + 2\mu \left[a(u_\epsilon, v) - L(v) \right] + \mu^2 a(v,v), \tag{13}$$

which means, using reformulation (12) that $\forall v \in H^m(\Omega, \mathbb{R}^n)$ and $\forall \mu \in \mathbb{R}$:

$$2\mu \left[a(u_\epsilon, v) - L(v) \right] + \mu^2 a(v,v) \geq 0. \tag{14}$$

Assuming that $\mu > 0$, dividing inequality (14) by μ and letting μ tend to zero, we finally get:

$$a(u_\epsilon, v) - L(v) \geq 0. \tag{15}$$

Assuming now that $\mu < 0$, one proves in a same way that:

$$a(u_\epsilon, v) - L(v) \leq 0, \tag{16}$$

from which we deduce that $a(u_\epsilon, v) = L(v)$, $\forall v \in H^m(\Omega, \mathbb{R}^n)$.

The converse is readily obtained thanks to relation (13) and the V-ellipticity of a which is proved afterwards. ■

We now give a lemma that will be of interest in the following.

Lemma 2.2. *The mapping defined by:*

$$|| \cdot ||_{A,m,\Omega,\mathbb{R}^n} : \left\{ \begin{array}{l} H^m(\Omega, \mathbb{R}^n) \to \mathbb{R} \\ \\ f \mapsto ||f||_{A,m,\Omega,\mathbb{R}^n} = \left(\langle \rho(f) \rangle_N^2 + |f|_{m,\Omega,\mathbb{R}^n}^2 \right)^{\frac{1}{2}} = \left(\sum_{i=1}^N \langle f(a_i) \rangle_n^2 + |f|_{m,\Omega,\mathbb{R}^n}^2 \right)^{\frac{1}{2}} \end{array} \right. \tag{17}$$

is a Hilbert norm equivalent to the norm $||f||_{m,\Omega,\mathbb{R}^n}$ in $H^m(\Omega, \mathbb{R}^n)$ ($H^m(\Omega, \mathbb{R}^n)$ is endowed with the usual norm denoted by $|| \cdot ||_{m,\Omega,\mathbb{R}^n}$ and the associated semi-norm denoted by $| \cdot |_{m,\Omega,\mathbb{R}^n}$).

The proof of this lemma requires the use of Nečas' theorem (Chapter 2, section 7.1 from [36]) which states the following (the notations are those by Nečas'):

Theorem 2.3. *Let Ω be a domain such that*

$$v \in P^{k-1}(\Omega) \Rightarrow ||v||_{L^p(\Omega)} < \infty,$$

with $k \geq 1$ a natural integer and $p \geq 1$. Then there exist functionals, f_i, $i = 1, 2, \cdots, l$ on $W_p^{(k)}(\Omega)$ such that if $v \in P_{k-1}(\Omega)$, one has the equivalence:

$$\sum_{i=1}^{l} |f_i v|^p = 0 \Leftrightarrow v \equiv 0. \tag{18}$$

Let $\Omega \in \aleph^{(0)}$ (see [36]) and let f_i be functionals satisfying (18), $k \geq 1$ a natural integer and $p \geq 1$. One has the inequality:

$$c_1 ||u||_{W_p^{(k)}(\Omega)} \leq \left[\sum_{\alpha=k} ||D^\alpha u||_{L^p(\Omega)}^p + \sum_{i=1}^{l} |f_i u|^p \right]^{\frac{1}{p}} \leq c_2 ||u||_{W_p^{(k)}(\Omega)}. \tag{19}$$

Proof of Lemma 2.2

Let us take f such that $||f||_{A,m,\Omega,\mathbb{R}^n} = 0$. It implies that $|f|_{m,\Omega,\mathbb{R}^n} = 0$ and taking into account the connectedness of Ω, it yields $f \in P^{m-1}(\Omega, \mathbb{R}^n)$.
As the set A contains a P^{m-1}-unisolvent subset, we deduce that $f \equiv 0$.
It is now clear that $|| \cdot ||_{A,m,\Omega,\mathbb{R}^n}$ is a norm on $H^m(\Omega, \mathbb{R}^n)$ associated with a scalar product.
We now prove the equivalence of the norm $|| \cdot ||_{A,m,\Omega,\mathbb{R}^n}$ with the norm $|| \cdot ||_{m,\Omega,\mathbb{R}^n}$. First, we have:
$\forall f \in H^m(\Omega, \mathbb{R}^n)$, $\forall a_i \in A$, $i = 1, \cdots, N$,

$$\langle f(a_i) \rangle_n \leq ||f||_{\mathcal{C}^0(\bar{\Omega},\mathbb{R}^n)} \leq c||f||_{H^m(\Omega,\mathbb{R}^n)} (\text{ Sobolev's embedding })$$

$$\text{so, } ||f||_{A,m,\Omega,\mathbb{R}^n} \leq \ (1 + c^2 N)^{\frac{1}{2}} ||f||_{m,\Omega,\mathbb{R}^n}.$$

Let us take $k = m$ and $p = 2$ in Nečas' theorem and let us take ρ as functional f_i. Due to the property of unisolvence of the set A, ρ satisfies property (18). We then obtain from Nečas' theorem that there exists a positive constant c_1 such that:

$$||f||_{m,\Omega,\mathbb{R}^n} \leq \frac{1}{c_1} \left[|f|_{m,\Omega,\mathbb{R}^n}^2 + \sum_{i=1}^{N} \langle f(a_i) \rangle_n^2 \right]^{\frac{1}{2}} = \frac{1}{c_1} ||f||_{A,m,\Omega,\mathbb{R}^n},$$

which concludes the proof.

■

We now can establish the following theorem.

Theorem 2.4. *Variational problem (9) admits a unique solution.*

Proof

The mapping L defined in (11) is a linear form on $H^m(\Omega, \mathbb{R}^n)$, continuous on $H^m(\Omega, \mathbb{R}^n)$. Indeed,

$$\begin{aligned} |L(v)| = |\sum_{i=1}^{N} \langle w_i, v(a_i)\rangle_n| &\leq \sum_{i=1}^{N} |\langle w_i, v(a_i)\rangle_n|, \\ &\leq \sum_{i=1}^{N} \langle w_i\rangle_n \langle v(a_i)\rangle_n, \\ &\leq ||v||_{\mathcal{C}^0(\bar{\Omega}, \mathbb{R}^n)} \sum_{i=1}^{N} \langle w_i\rangle_n, \\ &\leq cN \max_{i=1,\cdots,N} \langle w_i\rangle_n \ ||v||_{H^m(\Omega,\mathbb{R}^n)}. \end{aligned}$$

Moreover, the mapping a is a symmetric, bilinear form, continuous on $H^m(\Omega, \mathbb{R}^n) \times H^m(\Omega, \mathbb{R}^n)$. While symmetry and bilinearity are obvious, the continuity of a can be obtained by using the equivalence of norms established above.
$\forall u, v \in H^m(\Omega, \mathbb{R}^n) \times H^m(\Omega, \mathbb{R}^n)$,

$$\begin{aligned} |a(u,v)| = |\sum_{i=1}^{N} \langle u(a_i), v(a_i)\rangle_n + \epsilon(u,v)_{m,\Omega,\mathbb{R}^n}|, \\ \leq \ \max(1,\epsilon) \ \left[\sum_{i=1}^{N} |\langle u(a_i), v(a_i)\rangle_n| + |(u,v)_{m,\Omega,\mathbb{R}^n}|\right], \\ \leq \ \max(1,\epsilon) \ \left[\sum_{i=1}^{N} \langle u(a_i)\rangle_n \langle v(a_i)\rangle_n + |u|_{m,\Omega,\mathbb{R}^n} |v|_{m,\Omega,\mathbb{R}^n}\right], \\ \leq \ \max(1,\epsilon) ||u||_{A,m,\Omega,\mathbb{R}^n} ||v||_{A,m,\Omega,\mathbb{R}^n}. \end{aligned}$$

This last inequality proves that a is continuous on $H^m(\Omega, \mathbb{R}^n) \times H^m(\Omega, \mathbb{R}^n)$.

To finish with, we prove that a is $H^m(\Omega, \mathbb{R}^n)$-elliptic.

Let v belongs to $H^m(\Omega, \mathbb{R}^n)$.

$$\begin{aligned} a(v,v) &= \langle \rho(v)\rangle_N^2 + \epsilon |v|_{m,\Omega,\mathbb{R}^n}^2 \\ &\geq \ \min(1,\epsilon) \ ||v||_{A,m,\Omega,\mathbb{R}^n}^2. \end{aligned}$$

Using once again the equivalence of norms established above, we deduce that a is $H^m(\Omega, \mathbb{R}^n)$-elliptic.

The Lax-Milgram theorem enables us to conclude that the variational problem (9) has a unique solution denoted by u_ϵ.

■

We now go back to the initial minimization problem (6). As previously stressed, this problem does not admit a unique solution since the potential is defined up to a constant. We have the following theorem.

Theorem 2.5. *If σ_ϵ^1 and σ_ϵ^2 are two distinct solutions of problem (6) then:*

$$\nabla\sigma_\epsilon^1 = \nabla\sigma_\epsilon^2 = u_\epsilon, \tag{20}$$

where u_ϵ is the unique solution of problem (8).

Proof

The minimization problem (6) is equivalent to the problem stated by:

$$\begin{cases} \text{Search for } \sigma_\epsilon \in H^{m+1}(\Omega,\mathbb{R}) \text{ such that} \\ \forall v \in H^{m+1}(\Omega,\mathbb{R}),\ \langle\rho(\nabla\sigma_\epsilon),\rho(\nabla v)\rangle_N + \epsilon(\nabla\sigma_\epsilon,\nabla v)_{m,\Omega,\mathbb{R}^n} = \langle w,\rho(\nabla v)\rangle_N. \end{cases} \tag{21}$$

Let σ_ϵ^1 and σ_ϵ^2 be two distinct solutions of problem (6) and therefore of problem (21).

σ_ϵ^1 verifies: $\forall v \in H^{m+1}(\Omega,\mathbb{R})$,

$$\langle\rho(\nabla\sigma_\epsilon^1),\rho(\nabla v)\rangle_N + \epsilon(\nabla\sigma_\epsilon^1,\nabla v)_{m,\Omega,\mathbb{R}^n} = \langle w,\rho(\nabla v)\rangle_N.$$

Let us take $v = \sigma_\epsilon^2 - \sigma_\epsilon^1$ as test function then the following holds:

$$\langle\rho(\nabla\sigma_\epsilon^1),\rho\left(\nabla\left(\sigma_\epsilon^2-\sigma_\epsilon^1\right)\right)\rangle_N + \epsilon\left(\nabla\sigma_\epsilon^1,\nabla\left(\sigma_\epsilon^2-\sigma_\epsilon^1\right)\right)_{m,\Omega,\mathbb{R}^n} = \langle w,\rho\left(\nabla\left(\sigma_\epsilon^2-\sigma_\epsilon^1\right)\right)\rangle_N. \tag{22}$$

In a same way, σ_ϵ^2 satisfies: $\forall v \in H^{m+1}(\Omega,\mathbb{R})$,

$$\langle\rho(\nabla\sigma_\epsilon^2),\rho(\nabla v)\rangle_N + \epsilon(\nabla\sigma_\epsilon^2,\nabla v)_{m,\Omega,\mathbb{R}^n} = \langle w,\rho(\nabla v)\rangle_N.$$

Taking as test function $v = \sigma_\epsilon^2 - \sigma_\epsilon^1$, we finally obtain:

$$\langle\rho(\nabla\sigma_\epsilon^2),\rho\left(\nabla\left(\sigma_\epsilon^2-\sigma_\epsilon^1\right)\right)\rangle_N + \epsilon\left(\nabla\sigma_\epsilon^2,\nabla\left(\sigma_\epsilon^2-\sigma_\epsilon^1\right)\right)_{m,\Omega,\mathbb{R}^n} = \langle w,\rho\left(\nabla\left(\sigma_\epsilon^2-\sigma_\epsilon^1\right)\right)\rangle_N. \tag{23}$$

Substracting (23) to (22), it yields:

$$\langle\rho\left(\nabla\left(\sigma_\epsilon^2-\sigma_\epsilon^1\right)\right)\rangle_N^2 + \epsilon|\nabla\left(\sigma_\epsilon^2-\sigma_\epsilon^1\right)|_{m,\Omega,\mathbb{R}^n}^2 = 0. \tag{24}$$

Thus $|\nabla\left(\sigma_\epsilon^2-\sigma_\epsilon^1\right)|_{m,\Omega,\mathbb{R}^n} = 0$.
Taking into account the connectedness of Ω, we deduce that $\sigma_\epsilon^2 - \sigma_\epsilon^1$ is a polynomial of degree m. Consequently, $\nabla\left(\sigma_\epsilon^2-\sigma_\epsilon^1\right) \in P^{m-1}(\Omega,\mathbb{R}^n)$. With the hypothesis of unisolvence, it follows that:

$$\nabla\sigma_\epsilon^1 = \nabla\sigma_\epsilon^2.$$

To complete the proof, if σ_ϵ is a solution of (6) (*equivalent to the variational problem (21)*) then $\sigma_\epsilon \in \mathcal{C}^1(\bar{\Omega}, \mathbb{R})$ and $\nabla\sigma_\epsilon \in H^m(\Omega, \mathbb{R}^n)$ verifies (8) (*equivalent to the variational problem (9)*) and from Th. 2.4, it comes:

$$\nabla\sigma_\epsilon = u_\epsilon.$$

■

3. A result of convergence

In the following, we consider classical convergence hypotheses (see [5] for more details).

Let D be a subset of $\mathbb{R}^{+*}$ for which 0 is an accumulation point.
For any $d \in D$, let A^d be a set of $N = N(d)$ distinct points from $\bar{\Omega}$ that contains a P^{m-1}-unisolvent subset. We assume that

$$\sup_{x\in\Omega} \delta(x, A^d) = d, \tag{25}$$

where δ is the Euclidean distance in $\mathbb{R}^n$. Thus d is the radius of the biggest sphere included in Ω that contains no point from A^d (*Hausdorff distance*).
Also d is bounded and

$$\lim_{d\to 0} \sup_{x\in\Omega} \delta(x, A^d) = 0. \tag{26}$$

For any $d \in D$, let us denote by ρ^d the mapping defined by:

$$\rho^d : \begin{cases} H^m(\Omega, \mathbb{R}^n) \to (\mathbb{R}^n)^N \\ \\ v \mapsto \rho^d(v) = \left((v(a))_{a\in A^d}\right)^T. \end{cases}$$

Introducing the norm $||\cdot||_{A^d,m,\Omega,\mathbb{R}^n}$ defined by:

$$||f||_{A^d,m,\Omega,\mathbb{R}^n} = \left[\langle\rho^d(f)\rangle_N^2 + |f|_{m,\Omega,\mathbb{R}^n}^2\right]^{\frac{1}{2}},$$

as shown in Lemma 2.2, the norm $||\cdot||_{A^d,m,\Omega,\mathbb{R}^n}$ is equivalent to the norm $||\cdot||_{m,\Omega,\mathbb{R}^n}$ in $H^m(\Omega, \mathbb{R}^n)$.

To prove the convergence result, we need the following lemma.

Lemma 3.1. *Let $A_0 = \{b_{01}, b_{02}, \cdots, b_{0\aleph}\}$ be a fixed P^{m-1}-unisolvent subset of $\bar{\Omega}$ (in this case, $\aleph = \dim\ P^{m-1}$).*
By hypothesis, $0 \in \bar{D}$ and (26) holds so:

$$\forall j = 1, \cdots, \aleph,\ \exists\ \left(a_{0j}^d\right)_{d\in D},\ \left(\forall d \in D,\ a_{0j}^d \in A^d\right)\quad \textit{and}\ \left(b_{0j} = \lim_{d\to 0} a_{0j}^d\right). \tag{27}$$

For any $d \in D$, let A_0^d be the set $\left\{a_{01}^d, \cdots, a_{0\aleph}^d\right\}$ and let $||\cdot||_{A_0^d,m,\Omega,\mathbb{R}^n}$ be the mapping defined by: $\forall f \in H^m(\Omega,\mathbb{R}^n)$,

$$||f||_{A_0^d,m,\Omega,\mathbb{R}^n} = \left[\sum_{j=1}^{\aleph} \langle f(a_{0j}^d)\rangle_n^2 + |f|_{m,\Omega,\mathbb{R}^n}^2\right]^{\frac{1}{2}}.$$

Then, there exists $\eta > 0$ such that for any $d \leq \eta$, the set A_0^d is P^{m-1}-unisolvent and $||\cdot||_{A_0^d,m,\Omega,\mathbb{R}^n}$ is a norm on $H^m(\Omega,\mathbb{R}^n)$ uniformly equivalent over $D\cap]0,\eta]$ to the norm $||\cdot||_{m,\Omega,\mathbb{R}^n}$.

Theorem 3.2. *Assume that there exists a function $\widehat{f} \in H^m(\Omega,\mathbb{R}^n)$ such that for any $d \in D$: $\rho^d(\widehat{f}) = w = w^d$ (we recall that $w = w^d$ is the given data set - a gradient vector set, that is, the input of our problem), and $\varepsilon = \varepsilon(d) \in]0,\varepsilon_0], \varepsilon_0 > 0$. For any $d \in D$, we denote by u_ε^d the unique solution of problem (8). Then under the above assumptions we have:*

$$\lim_{d\to 0} ||u_\varepsilon^d - \widehat{f}||_{m,\Omega,\mathbb{R}^n} = 0. \tag{28}$$

Proof
The proof is made using compactness arguments and norm equivalences and can be found in [25].

4. Datasets stemming from registration processes

In the following applications, the resulting vector field u_ϵ is such that $T(\varphi)$ with φ the deformation defined by $\varphi = \mathrm{Id} + u_\epsilon$ is close to R in terms of intensities. In the first example, we consider the problem of warping a black disk to the letter C both defined on the same image domain (Fig. 1). The input of our problem is the discrete vector field obtained at an intermediate step of the registration process. The given set of vectors is regularly distributed on the domain Ω and natu-

Figure 1: On the left, the reference image R. On the right, the template image T.

rally, the cardinal number of this set (6084) is related to the size of the studied image domain. The triangulation of the domain Ω is made up of 10×10 equal squares and so $M_h = 4 \times 11^2 = 484$. The given set of vectors $\{w_i\}_{i=1,\cdots,N}$ is depicted in Fig. 2. Also, this figure is complemented by the plots of each component of the vector field, Fig. 3. The finite element space V_h is constructed on the triangulation from the Bogner-Fox-Schmit rectangle of class $\mathcal{C}^1$ and the corresponding approximant u_ϵ^h is computed. The results are presented in Fig. 4-6. We have used a mesh refinement for the visualization: each square has been subdivided into 15×15 equal squares. The relative

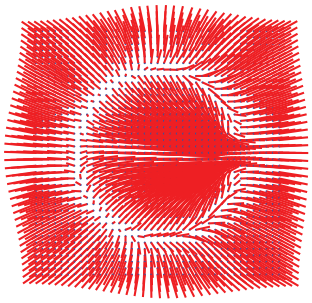

Figure 2: Plot of the given vector field $\{w_i\}_{i=1,\cdots,N}$ (every two rows and columns). The blue diamond indicates the point to which the vector is attached.

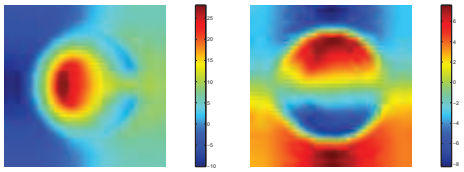

Figure 3: On the left, plot of the first component of the vector field $\{w_i\}_{i=1,\cdots,N}$. On the right, plot of the second component.

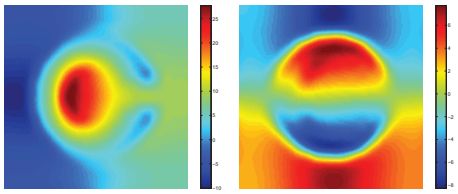

Figure 4: On the left, plot of the first component of the obtained vector field. On the right, plot of the second component.

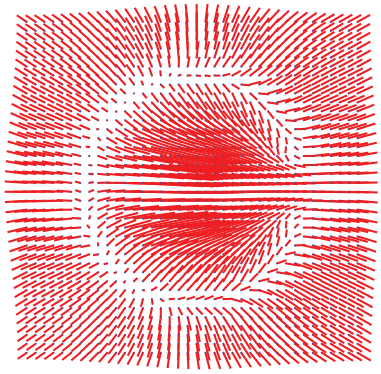

Figure 5: Plot of the obtained vector field (every four rows and columns). The blue diamond indicates the point to which the vector is attached.

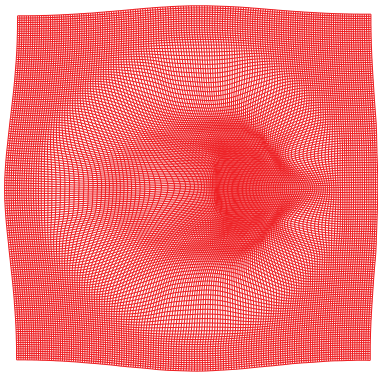

Figure 6: Alternative way of visualization of the vector field as a mesh.

error is equal to 0.0138484627.

The second example is related to a medical application which aims at mapping mouse gene data to an atlas. The input of our problem is the discrete vector field obtained at the end of the registration process. The given set of vectors is regularly distributed on the domain Ω and naturally, the cardinal number of this set (40000) is related to the size of the studied image domain. The triangulation of the domain Ω is made up of 15×15 equal squares and so $M_h = 4 \times 16^2 = 1024$. The given set of vectors $\{w_i\}_{i=1,\cdots,N}$ is depicted in Fig. 7. Also, this figure is complemented by the plots of each component of the vector field, Fig. 8. The finite element space V_h is constructed on the triangulation from the Bogner-Fox-Schmit rectangle of class $\mathcal{C}^1$ and the corresponding approximant u_ϵ^h is computed. The results are presented in Fig. 9-11. We have used a mesh refinement for the visualization: each square has been subdivided into 20×20 equal squares. The relative error is equal to 0.0285239131.

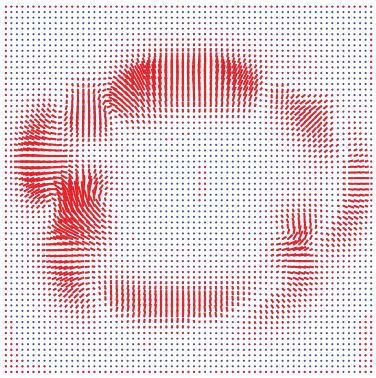

Figure 7: Plot of the given vector field $\{w_i\}_{i=1,\cdots,N}$ (every three rows and columns). The blue diamond indicates the point to which the vector is attached.

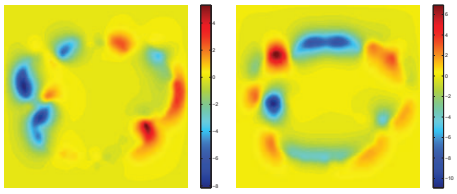

Figure 8: On the left, plot of the first component of the vector field $\{w_i\}_{i=1,\cdots,N}$. On the right, plot of the second component.

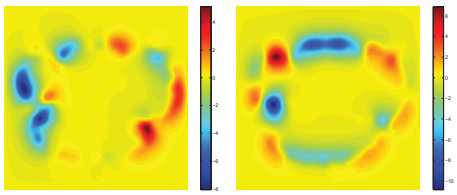

Figure 9: On the left, plot of the first component of the obtained vector field. On the right, plot of the second component.

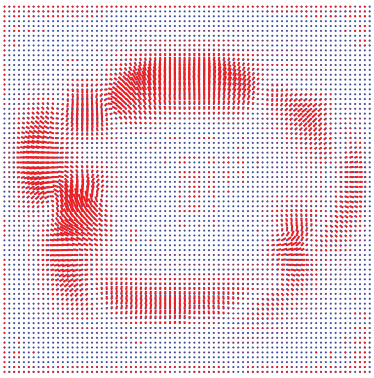

Figure 10: Plot of the obtained vector field (every four rows and columns). The blue diamond indicates the point to which the vector is attached.

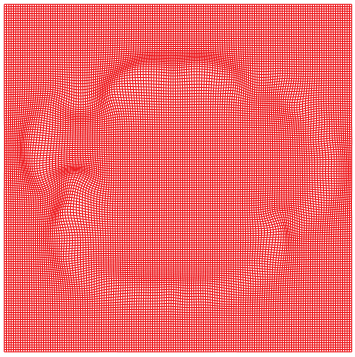

Figure 11: Alternative way of visualization of the vector field as a mesh.

The last proposed example is drawn from the registration of a disk to a triangle. The input of our problem is the discrete vector field obtained at the end of the registration process. The given set of vectors is regularly distributed on the domain Ω and naturally, the cardinal number of this set (2700) is related to the size of the studied image domain. The triangulation of the domain Ω is made up of 12×12 rectangles and so $M_h = 4 \times 13^2 = 676$. The given set of vectors $\{w_i\}_{i=1,\cdots,N}$ is depicted in Fig. 12. Also, this figure is complemented by the plots of each component of the vector field, Fig. 13. The finite element space V_h is constructed on the triangulation from the Bogner-Fox-Schmit rectangle of class $\mathcal{C}^1$ and the corresponding approximant u_ϵ^h is computed. The results are presented in Fig. 14-16. We have used a mesh refinement for the visualization: each rectangle has been subdivided into 15×15 rectangles. The relative error is equal to 0.0378234465.

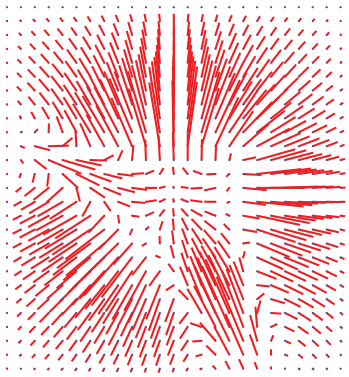

Figure 12: Plot of the given vector field $\{w_i\}_{i=1,\cdots,N}$ (every two rows and columns). The blue diamond indicates the point to which the vector is attached.

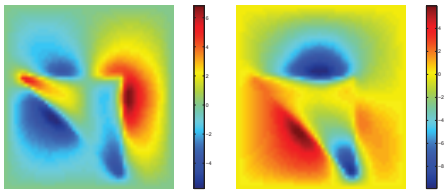

Figure 13: On the left, plot of the first component of the vector field $\{w_i\}_{i=1,\cdots,N}$. On the right, plot of the second component.

5. Conclusion

In this paper, we have addressed the issue of vector field approximation. The problem is phrased as a functional minimization problem for which we have provided existence and uniqueness of the

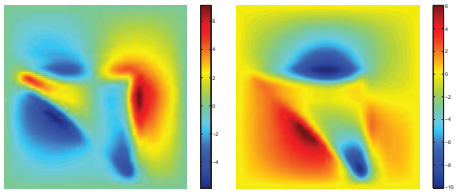

Figure 14: On the left, plot of the first component of the obtained vector field. On the right, plot of the second component.

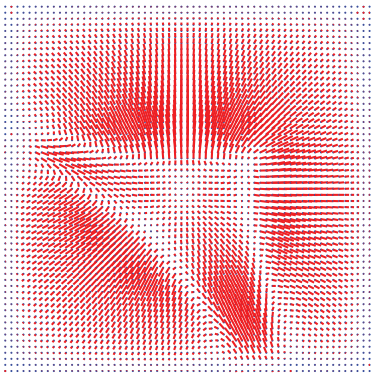

Figure 15: Plot of the obtained vector field (every three rows and columns). The blue diamond indicates the point to which the vector is attached.

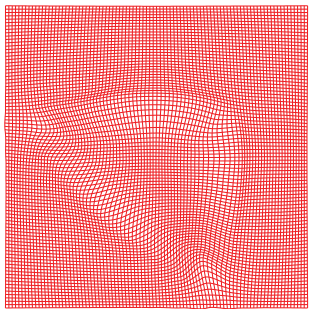

Figure 16: Alternative way of visualization of the vector field as a mesh.

solution. A convergence result has been established when the radius of the biggest sphere included in Ω that contains no point from A^d tends to zero. The discretization stage is made using the finite element method and is complemented by numerical experiments both on synthetic datasets and on real data stemming in particular from image registration processes. These illustrate the efficiency of the method that globally captures a good approximant.

Acknowledgement.
The first author would like to thank Jan Modersitzki and Hemant Tagare for their useful suggestions about visualization.

References

[1] L. Alvarez, F. Guichard, P.L. Lions and J.M. Morel, *Axioms and fundamental equations of image processing*, Arch. Rational Mechan. Anal., 16 (IX), 200–257, 1993.

[2] L. Amodei and M.N. Benbourhim, *A Vector Spline Approximation*, Journal of Approximation Theory, 67(1), 51–79, 1991.

[3] D. Apprato and C. Gout, *A result about scale transformation families in approximation: application to surface fitting from rapidly varying data*, Numerical Algorithms, 23 (2-3), 263–279, 2000.

[4] D. Apprato, C. Gout and D. Komatitsch, *Surface fitting from ship track data : application to the bathymetry of the Marianas trench*, Math. Geol., 34(7), 831–843, 2002.

[5] R. Arcangéli, M.C. López de Silanes and J.J. Torrens, *Multidimensional minimizing splines. Theory and applications*, Grenoble Sciences, Kluwer Academic Publishers, Boston, MA, 2004, xvi+261 pp., ISBN: 1-4020-7786-6.

[6] G. Awanou and M. J. Lai, *Trivariate spline approximations of 3D Navier-Stokes equations*, Math. Comp., 74, 585–601, 2005.

[7] M.N. Benbourhim and A. Bouhamidi, *Approximation of vector fields by thin plate splines with tension*, Journal of Approximation Theory, 136, 198–229, 2005.

[8] M.N. Benbourhim and A. Bouhamidi, *Pseudo-polyharmonic vectorial approximation for div-curl and elastic semi-norms*, Numerische Mathematik, 109(3), 333–364, 2008.

[9] C. Broit, *Optimal Registration of Deformed Images*, PhD thesis, Computer and Information Science, University of Pennsylvania, 1981.

[10] V. Caselles, J.M. Morel and C. Sbert, *An Axiomatic Approach to Image Interpolation*, IEEE Transactions on Image Processing, 7(3), 376–386, 1998.

[11] A. Chessel, F. Cao and R. Fablet, *Interpolating Orientation Fields: An Axiomatic Approach*, In Proc. European Conf. Comp. Vision (ECCV'06), Volume 3951 (LNCS), 241–254, Graz, Austria, May 2006.

[12] G.E. Christensen, R.D. Rabbitt and M.I. Miller, *Deformable Templates Using Large Deformation Kinematics*, IEEE Trans. Image Process., 5(10), 1435–1447, 1996.

[13] F. Dodu and C. Rabut, *Vectorial interpolation using radial-basis-like functions*, Comput. Math. Appl., 43(3-5), 393–411, 2002.

[14] M. Droske and M. Rumpf, *A variational approach to non-rigid morphological registration*, SIAM J. Appl. Math., 64(2), 668–687, 2004.

[15] J. Duchon, *Splines minimizing rotation-invariant semi-norms in Sobolev spaces*, In Constructive Theory of Functions of Several Variables, W. Schempp, K. Zeller (eds.), Lecture Notes in Mathematics, 571, 85–100, Spinger Berlin, 1977.

[16] A.S. Dzhabrailov, Y.V. Klochkov, S.S. Marchenko and A.P. Nikolaev, *The finite element approximation of vector fields in curvilinear coordinates*, Russian Aeronautics (Iz VUZ), 50(2), 115–120, 2007.

[17] S. Ettl-Lowitzsch, J. Kaminski, M.C. Knauer, and G. Häusler, *Shape reconstruction from gradient data*, Applied Optics, 47(12), 2091–20971, 2008.

[18] B. Fischer and J. Modersitzki, *Fast Diffusion Registration*, AMS Contemporary Mathematics, Inverse Problems, Image Analysis, and Medical Imaging, 313, 117–129, 2002.

[19] B. Fischer and J. Modersitzki, *Curvature based image registration*, JMIV, 18(1), 81–85, 2003.

[20] B. Fischer and J. Modersitzki, *A Unified Approach to Fast Image Registration and a New Curvature Based Registration Technique*, Linear Algebra and its applications, 380, 107–124, 2004.

[21] C. Gout, *C^k surface reconstruction from surface patches*, Computers & Mathematics with Applications, 44(3-4), 389–406, 2002.

[22] N. Jifeng, W. Chengke, L. Shigang and Y. Shuqin, *NGVF: An improved external force field for active contour model*, Pattern Recognition Letters, 28, 58–63, 2007.

[23] Y. Kuroe, M. Mitsui, H. Kawakami and T. Mori, *A Learning Method for Vector Field Approximation by Neural Networks*, IEEE World Congress on Computational Intelligence, 3, 2300–2305, 1998.

[24] C. Le Guyader and L. Vese, *A Combined Segmentation and Registration Framework with a Nonlinear Elasticity Smoother*, UCLA CAM Report 08-16, 2008.

[25] C. Le Guyader, D. Apprato and C. Gout, *Spline approximation of gradient fields: application to wind vector fields*, submitted, 2011.

[26] C. Le Guyader and L. Guillot, *Extrapolation of vector fields using the infinity Laplacian and with applications to image segmentation*, Communications in Math. Sci, to appear.

[27] S. Lowitzsch, *Approximation and Interpolation employing divergence-free radial basis functions with applications*, Dissertation, Texas A&M University, 2002.

[28] S. Lowitzsch, *Error estimate for matrix-valued radial basis functions interpolation*, J. Approx. Theory, 137(2), 238–249, 2005.

[29] M.C. López de Silanes, R. Arcangéli, *Estimations de l'erreur d'approximation par splines d'interpolation et d'ajustement d'ordre* (m, s)*, (French) [Approximation error estimates for interpolating and smoothing* (m, s)*-splines]*, Numer. Math., 56(5), 449–467, 1989.

[30] M.C. López de Silanes, R. Arcangéli, *Sur la convergence des* D^m*-splines d'ajustement pour des données exactes ou bruitées, (French) [On the convergence of fitting* D^m*-splines for exact or noisy data]*, Rev. Mat. Univ. Complut. Madrid, 4(2-3), 279–294, 1991.

[31] M. Lage, F. Petronetto, A. Paiva, H. Lopes, T. Lewiner and G. Tavares, *Vector field reconstruction from sparse samples with applications*, SIBGRAPI 2006, 297–306, 2006.

[32] S. Lowitzsch, *Approximation and Interpolation employing divergence-free radial basis functions with applications*, Dissertation, Texas A&M University, 2002.

[33] J. Modersitzki, *Numerical Methods for Image Registration*, Oxford University Press, 2004.

[34] L. Monier, F. Brossier and F. Razafimahery, *Dynamic of the currents in the Mozambique canal*, Proceedings of the 30^{th} Jubilee International Conference on Applications of Mathematics in Engineering and Economics, 130–135, 2004.

[35] J.M. Morvan and B. Thibert, *On The Approximation Of The Normal Vector Field Of A Smooth Surface*, Research Report 4476, INRIA, 2002.

[36] J. Nečas, *Les méthodes directes en théorie des équations elliptiques*, Paris, Masson, 1967.

[37] K. Polthier and E. Preuss, *Variational Approach to Vector Field Decomposition*, Scientific Visualization, Springer Verlag (Proc. of Eurographics Workshop on Scientific Visualization), 9p., 2000.

[38] C. Xu and J.L. Prince, *Snakes, shapes, and gradient vector flow*, IEEE Trans. Image Process., 7(3), 359–369, 1998.